

Provided for non-commercial research and education use.
Not for reproduction, distribution or commercial use.



(This is a sample cover image for this issue. The actual cover is not yet available at this time.)

This article appeared in a journal published by Elsevier. The attached copy is furnished to the author for internal non-commercial research and education use, including for instruction at the authors institution and sharing with colleagues.

Other uses, including reproduction and distribution, or selling or licensing copies, or posting to personal, institutional or third party websites are prohibited.

In most cases authors are permitted to post their version of the article (e.g. in Word or Tex form) to their personal website or institutional repository. Authors requiring further information regarding Elsevier's archiving and manuscript policies are encouraged to visit:

<http://www.elsevier.com/copyright>



Contents lists available at SciVerse ScienceDirect

International Journal of Heat and Mass Transfer

journal homepage: www.elsevier.com/locate/ijhmt

A similarity theory for natural convection from a horizontal plate for prescribed heat flux or wall temperature

Subho Samanta, Abhijit Guha*

Mechanical Engineering Department, Indian Institute of Technology Kharagpur, Kharagpur 721302, India

ARTICLE INFO

Article history:

Received 30 March 2011

Received in revised form 1 February 2012

Accepted 8 February 2012

ABSTRACT

An analysis is performed to study the fluid flow and heat transfer characteristics for the steady laminar natural convection boundary layer flow over a semi-infinite horizontal flat plate subjected to a variable heat flux or variable wall temperature. The heat flux $q_w(\bar{x})$ varies as the power of the horizontal coordinate in the form $q_w(\bar{x}) = a\bar{x}^m$ whereas the wall temperature $T_w(\bar{x})$ is assumed to vary as $T_w(\bar{x}) = T_\infty + b\bar{x}^n$. The governing boundary layer equations are first cast into a dimensionless form and then transformed to ordinary differential equations using generalized stretching transformation to derive the appropriate similarity variables. This results in a set of three coupled, non-linear ordinary differential equations with variable coefficients (representing the interaction of the temperature and velocity fields) which are then solved by the shooting method. The numerical results are obtained for various values of Prandtl number under different levels of heating. The effects of various values of Prandtl number and the indices m and n on the velocity profiles, temperature profiles, skin friction, and heat transfer coefficients are presented. Correlation equations between Nusselt number and Grashof number, and that between skin friction coefficient and Grashof number have been derived. It is shown that when the heat flux variation is specified, $Nu \propto (Gr_T)^{\frac{1}{2}}$ and $\hat{c}_f \propto (Gr_T)^{-\frac{1}{2}}$; when the wall temperature variation is specified, $Nu \propto (Gr_T)^{\frac{1}{2}}$ and $\hat{c}_f \propto (Gr_T)^{-\frac{1}{2}}$. For a fixed value of m or n (including the cases of constant wall temperature or constant heat flux), the heat transfer coefficient increases whereas the local wall shear stress decreases with increasing Prandtl number. The heat transfer coefficient increases with increasing values of exponent m or n when the Prandtl number is kept constant. For a fixed Prandtl number, the local wall shear stress increases with increasing values of n , while it decreases with increasing values of m .

© 2012 Elsevier Ltd. All rights reserved.

1. Introduction

Transport of heat by natural convection arises in nature and many engineering applications. The bulk fluid motion in this case is generated only by density differences in the fluid occurring due to temperature gradients. Applications include cooling of electronic equipments, heat transfer from refrigeration coils, heat loss from power transmission lines, heat transfer from human and animal bodies, etc. Thus the phenomenon of natural convection has been studied extensively.

Experimental and analytical study of laminar free convection from a vertical plate with both constant surface temperature and constant wall heat flux is given in Rajan and Picot [1], Burmeister [2], Martynenko et al. [3], and Martynenko and Khramtsov [4]. Natural convection from a vertical flat plate with uniform surface temperature in a non-Newtonian fluid has been studied by Sharma and Adelman [5], and Ghosh Moulic and Yao [6].

Kurdyumov [7] presented steady, two-dimensional, laminar free convection flow downstream of a heat source near a horizontal or vertical wall at large Grashof numbers. Goldstein and Lau [8] performed an experimental and numerical study of laminar free convection from an isothermal horizontal plate, with particular attention on the effects of various plate-edge extensions. Kuiken [9] presented an analysis of free convection boundary layer by the method of matched asymptotic expansion for fluids with low Prandtl number.

Natural convection from horizontal plates has not been studied analytically as extensively as compared to the case of vertical plates. Clifton and Chapman [10] analytically solved boundary layer equations by integral analysis to determine the heat transfer from a finite size isothermal horizontal plate with the cold face facing upwards. Pretot et al. [11] numerically and experimentally studied heat transfer in laminar free convection above an upward facing horizontal heated plate placed in a semi-infinite medium. Higher order natural convection boundary layer effects over a horizontal plate have been studied by Mahajan and Gebhart [12], and Afzal [13]. Schlichting and Gersten [14] have presented a similarity solution for horizontal semi-infinite plates for constant wall

* Corresponding author. Tel.: +91 3222 281768; fax: +91 3222 282278.

E-mail address: a.guha@mech.iitkgp.ernet.in (A. Guha).

Nomenclature

<p>a dimensional constant in the power-law variation of wall heat flux</p> <p>b dimensional constant in the power-law variation of wall temperature</p> <p>$C_{f\bar{x}}$ local skin friction coefficient</p> <p>\hat{C}_f average skin friction coefficient</p> <p>F, f reduced non-dimensional stream functions defined, respectively, by Eqs. (22) and (43)</p> <p>\bar{g} gravitational acceleration</p> <p>G, g reduced non-dimensional temperatures defined, respectively, by Eqs. (22) and (43)</p> <p>$Gr_{\bar{x}}, Gr_L$ Grashof numbers defined, respectively, as $\bar{g}\beta[\bar{T}_w(\bar{x}) - \bar{T}_\infty]\bar{x}^3/\nu^2$ and $\bar{g}\beta[\bar{T}_w(L) - \bar{T}_\infty]L^3/\nu^2$</p> <p>$Gr_{\bar{x}}^*, Gr_L^*$ modified Grashof numbers defined, respectively, as $[\bar{g}\beta q_w(\bar{x})\bar{x}^4]/(k\nu^2)$ and $[\bar{g}\beta q_w(L)L^4]/(k\nu^2)$</p> <p>$h$ local heat transfer coefficient, $q_w(\bar{x})/[\bar{T}_w(\bar{x}) - \bar{T}_\infty]$</p> <p>$\hat{h}$ average heat transfer coefficient defined by Eq. (39)</p> <p>k thermal conductivity of the fluid</p> <p>L reference length of the plate in \bar{x} direction</p> <p>m exponent in the power-law variation of wall heat flux</p> <p>n exponent in the power-law variation of wall temperature</p> <p>$Nu_{\bar{x}}$ local Nusselt number, $h\bar{x}/k$</p> <p>\hat{Nu} average Nusselt number, $\hat{h}L/k$</p> <p>\bar{p}_∞ static pressure in the undisturbed fluid</p> <p>p, p_{wt} non-dimensional static pressure difference defined in Eq. (6) and (41) respectively</p> <p>Pr Prandtl number, ν/α</p> <p>\bar{T} fluid temperature</p> <p>\bar{u} axial velocity component</p> <p>\bar{u}_0, \bar{u}_{0wt} velocity scales used to non-dimensionalize \bar{u} and \bar{v} in Eqs. (6) and (41) respectively</p> <p>u, u_{wt} non-dimensional axial velocity component defined in Eqs. (6) and (41) respectively</p> <p>\bar{v} normal velocity component</p>	<p>v, v_{wt} non-dimensional normal velocity component defined in Eqs. (6) and (41), respectively</p> <p>\bar{v} non-dimensional normal velocity component defined in Eq. (A1)</p> <p>\bar{x} axial coordinate</p> <p>x non-dimensional axial coordinate defined in Eqs. (6) and (41), respectively</p> <p>\bar{y} normal coordinate</p> <p>y non-dimensional normal coordinate defined in Eqs. (6) and (41), respectively</p> <p>\bar{y} non-dimensional normal coordinate defined in Eq. (A1)</p> <p>Greek symbols</p> <p>α thermal diffusivity</p> <p>β coefficient of thermal expansion at the reference temperature</p> <p>δ, δ_{wt} length scales used to non-dimensionalize normal coordinate \bar{y} in Eqs. (6) and (41), respectively</p> <p>η, η_{wt} similarity variables defined respectively by Eqs. (22) and (43), respectively</p> <p>μ dynamic viscosity</p> <p>ν kinematic viscosity</p> <p>θ, θ_t non-dimensional temperatures defined respectively by Eqs. (6) and (41), respectively</p> <p>ρ density of fluid</p> <p>τ_w local wall shear stress, $\mu(\partial\bar{u}/\partial\bar{y})_{\bar{y}=0}$</p> <p>$\psi$ non-dimensional stream function</p> <p>Subscripts</p> <p>w condition at the wall</p> <p>∞ condition in undisturbed fluid</p> <p>wt for the case when wall temperature is fixed</p> <p>Superscripts</p> <p>' differentiation with respect to η</p>
--	---

temperature. According to Schlichting and Gersten, the first similarity solution for an isothermal, semi-infinite, horizontal plate was given by Stewartson [15], later corrected by Gill et al. [16]. Experimental study of this problem is presented by Rotem and Claassen [17]. Schlichting and Gersten [14] termed this type of flow as “indirect natural convection”, for which, unlike the usual analysis for the boundary layer, neither the term $\partial p/\partial x$ nor the term $\partial p/\partial y$ can be neglected. The similarity solution provided in the present work for horizontal plates for the constant heat flux condition is believed to be the only of its kind. The present work also uses a generalized stretching transformation technique by which the process of identifying the appropriate similarity variables becomes systematized. Moreover, many engineering heat transfer applications involve cases of laminar natural convection where the surface temperature or heat flux is not constant. Similarity solutions for horizontal plates have been derived in the present work for both cases of variable surface temperature ($\bar{T}_w(\bar{x}) = \bar{T}_\infty + b\bar{x}^n$) and variable heat flux ($q_w(\bar{x}) = a\bar{x}^m$).

Similarity theory for an isothermal horizontal plate is the most readily available solution in the existing literature and is included in the book by Schlichting and Gersten [14]. Gebhart et al. [18] have presented more generalized similarity equations for natural convection along a semi-infinite horizontal flat plate with power law variation in wall temperature, but they directly quote the final

three ordinary differential equations only and no numerical computations are presented (numerical results for non-dimensional velocity and temperature profiles are given by Gebhart et al. [18] only for the case of isothermal horizontal plate which are the same as given by Schlichting and Gersten [14]).

A large number of important practical and experimental free convection situations correspond to cases where the surface dissipates heat non-uniformly rather than it is maintained at a non-uniform temperature. Chen et al. [19] studied the effect of laminar natural convection on horizontal and vertical plates for cases where either the surface temperature or the heat flux varies as a power of \bar{x} , but their solution involves an integro-differential approach. A similarity theory has been developed here. The present work is also more general than Chen et al. [19] in its applicability to fluids of various Prandtl numbers. In the present work we have considered the spectrum of Prandtl number from very low to very high, Prandtl number of liquid metals being less than 0.01 whereas that for heavy oils being more than 100,000. Numerical results are presented for a wide range of Prandtl numbers under different levels of heating.

Correlation equations for the local and average Nusselt number as well as those for local and average skin friction coefficient are also theoretically derived here. Chen et al. [19] have given correlations for Nusselt number alone but these seem to involve

$$\frac{c_2 c_3}{c_1^2} \left[\frac{\partial \psi^*}{\partial y^*} \frac{\partial^2 \psi^*}{\partial x^* \partial y^*} - \frac{\partial \psi^*}{\partial x^*} \frac{\partial^2 \psi^*}{\partial y^{*2}} \right] = -\frac{c_2}{c_5} \frac{\partial p^*}{\partial x^*} + \frac{c_3^3}{c_1} \frac{\partial^3 \psi^*}{\partial y^{*3}}, \quad (14)$$

$$-\frac{c_3}{c_5} \frac{\partial p^*}{\partial y^*} + \frac{1}{c_4} \theta^* = 0, \quad (15)$$

$$\frac{c_2 c_3}{c_1 c_4} \left[\frac{\partial \psi^*}{\partial y^*} \frac{\partial \theta^*}{\partial x^*} - \frac{\partial \psi^*}{\partial x^*} \frac{\partial \theta^*}{\partial y^*} \right] = \frac{1}{Pr} \frac{c_3^2}{c_4} \frac{\partial^2 \theta^*}{\partial y^{*2}}. \quad (16)$$

Boundary conditions:

$$\text{at } y^* = 0, \quad \frac{\partial \psi^*}{\partial y^*} = 0, \quad \frac{\partial \psi^*}{\partial x^*} = 0, \quad \frac{c_3}{c_4} \frac{\partial \theta^*}{\partial y^*} = -c_2^{-m} x^{*m}, \quad (17)$$

$$\text{as } y^* \rightarrow \infty, \quad \frac{\partial \psi^*}{\partial y^*} \rightarrow 0, \quad \theta^* \rightarrow 0, \quad p^* \rightarrow 0.$$

The boundary layer equations along with their boundary conditions should remain invariant under the special stretching transformation. Hence:

$$c_2 = c_1 c_3, \quad c_3^2 = \frac{c_1^2}{c_5}, \quad c_3 = c_4 c_2^{-m}, \quad c_5 = c_3 c_4. \quad (18)$$

Using Eq. (18) and expressing c_2, c_3, c_4, c_5 in terms of c_1 one obtains:

$$c_2 = \frac{6}{c_1^{(m+4)}}, \quad c_3 = \frac{(2-m)}{c_1^{(m+4)}}, \quad c_4 = \frac{(2+5m)}{c_1^{(m+4)}} \quad \text{and} \quad c_5 = \frac{(4+4m)}{c_1^{(m+4)}}. \quad (19)$$

Using Eq. (19), Eq. (13) can be rewritten as:

$$\psi^* = c_1 \psi, \quad x^* = c_1^{\frac{6}{(m+4)}} x, \quad y^* = c_1^{\frac{(2-m)}{(m+4)}} y, \quad p^* = c_1^{\frac{(4+4m)}{(m+4)}} p \quad \text{and} \quad \theta^* = c_1^{\frac{(2+5m)}{(m+4)}} \theta. \quad (20)$$

Eq. (20) shows that the PDEs along with their boundary conditions would become independent of c_1 for the following combinations of the variables:

$$\frac{y}{x^{\frac{(2-m)}{6}}}, \quad \frac{\psi}{x^{\frac{(m+4)}{6}}}, \quad \frac{\theta}{x^{\frac{(5m+2)}{6}}}, \quad \frac{p}{x^{\frac{(4m+4)}{6}}}. \quad (21)$$

Hence the appropriate similarity variable η and the functional forms for ψ, θ and p can then be written as:

$$\eta = Ayx^{\frac{(m-2)}{6}}, \quad \psi = Bx^{\frac{(m+4)}{6}} F(\eta), \quad \theta = Cx^{\frac{(5m+2)}{6}} G(\eta), \quad p = Dx^{\frac{(4m+4)}{6}} H(\eta), \quad (22)$$

where A, B, C and D are constants. With the help of Eq. (22), the boundary layer equations are transformed into the following ordinary differential equations:

$$F'''(\eta) - \frac{D}{3A^3 B} \left[2(m+1)H(\eta) + \frac{1}{2}(m-2)\eta H'(\eta) \right] = \frac{B}{3A} \left[(m+1)(F'(\eta))^2 - (m+4)\frac{1}{2}F(\eta)F''(\eta) \right], \quad (23)$$

$$-H'(\eta) + \frac{C}{AD} G(\eta) = 0, \quad (24)$$

$$\frac{ABC}{6} [(5m+2)F'(\eta)G(\eta) - (m+4)F(\eta)G'(\eta)] = \frac{1}{Pr} A^2 C G''(\eta). \quad (25)$$

The boundary conditions corresponding to Eqs. (23)–(25) are:

$$\text{at } \eta = 0, \quad F'(0) = F(0) = 1 + AC G'(0) = 0, \quad \text{and at } \eta \rightarrow \infty, \quad F'(\infty) = G(\infty) = H(\infty) = 0. \quad (26)$$

Choice of the constants A, B, C and D :

The choice of A, B, C and D are arbitrary and the simplest possible choice can be set $A = B = C = D = 1$. However, then Eqs. (23)–(25) will contain several constant coefficients. So here we choose values of A, B, C and D such that the Eqs. (23)–(25) contain the least number of constant coefficients.

Thus by setting:

$$\frac{D}{3A^3 B} = 1, \quad \frac{C}{AD} = 1, \quad \frac{B}{6A} = 1, \quad AC = 1, \quad (27)$$

A, B, C and D can be obtained as

$$A = \frac{1}{18^{\frac{1}{6}}}, \quad B = \frac{6}{18^{\frac{1}{6}}}, \quad C = 18^{\frac{1}{6}}, \quad D = 18^{\frac{1}{3}}. \quad (28)$$

Thus the following system of non-linear coupled ordinary differential equations with variable coefficients are obtained as the boundary layer equations:

$$F''' - 2 \left[(m+1)F'^2 - (m+4)\frac{1}{2}FF'' \right] - \left[2(m+1)H + \frac{1}{2}(m-2)\eta H' \right] = 0, \quad (29)$$

$$G - H' = 0, \quad (30)$$

$$\frac{1}{Pr} G'' - [(5m+2)F'G - (m+4)FG'] = 0. \quad (31)$$

The corresponding boundary conditions are:

$$\text{at } \eta = 0 \quad \text{and} \quad \eta \rightarrow \infty, \quad F'(0) = F(0) = 1 + G'(0) = F'(\infty) = G(\infty) = H(\infty) = 0, \quad (32)$$

where prime denotes differentiation with respect to η .

The local heat transfer coefficient (h) obtained by using expressions for θ from Eqs. (6) and (22) is given by

$$h = \frac{q_w(\bar{x})}{(T_w - T_\infty)} = \frac{k}{L} \frac{q_w(\bar{x})}{q_w(L)} \frac{1}{C G(0) x^{\frac{5m+2}{6}}} (Gr_L^*)^{\frac{1}{6}}. \quad (33)$$

The local Nusselt number $Nu_{\bar{x}}$ is given by

$$Nu_{\bar{x}} = \frac{h\bar{x}}{k} = \frac{1}{(18)^{\frac{1}{6}} G(0)} (Gr_{\bar{x}}^*)^{\frac{1}{6}}. \quad (34)$$

The local wall shear stress τ_w is given by $\tau_w = (\mu \frac{\partial u}{\partial y})_{y=0}$, where μ is the dynamic viscosity of the fluid. Using expressions for \bar{u}, u and ψ from Eqs. (6), (12), and (22) respectively the wall shear stress becomes:

$$\tau_w = \frac{6}{(18)^{\frac{1}{2}}} \frac{\mu \nu}{\bar{x}^2} (Gr_{\bar{x}}^*)^{\frac{1}{2}} F''(0). \quad (35)$$

The local skin friction coefficient, $c_{f\bar{x}}$, is defined as $c_{f\bar{x}} = \frac{\tau_w}{(1/2)\rho u_0^2} = \frac{\tau_w}{(1/2)\rho(\nu^2/L^2)(Gr_L^*)^{\frac{2}{3}}}$. Substituting the value of τ_w from Eq. (35), the expression for local skin friction coefficient becomes:

$$c_{f\bar{x}} = \frac{12}{(18)^{\frac{1}{2}}} x^{\frac{2}{3}(m+1)} (Gr_{\bar{x}}^*)^{-\frac{1}{6}} F''(0). \quad (36)$$

The average skin friction coefficient (\hat{c}_f) is given by

$$\hat{c}_f = \frac{1}{L} \int_0^L c_{f\bar{x}} d\bar{x} = \int_0^1 c_{f\bar{x}} dx. \quad (37)$$

Substituting the value of $c_{f\bar{x}}$ from Eq. (36) the average skin friction coefficient (\hat{c}_f) may be written as:

$$\hat{c}_f = \frac{24}{(18)^{\frac{1}{2}} (m+2)} (Gr_L^*)^{-\frac{1}{6}} F''(0). \quad (38)$$

The average heat transfer coefficient (\hat{h}) may be written as

$$\hat{h} = \frac{1}{L} \int_0^L h d\bar{x} = \int_0^1 h dx. \quad (39)$$

Using the expression for local heat transfer coefficient from Eq. (33), the average Nusselt number (Nu) over a plate length of L is:

$$\hat{Nu} = \frac{6}{m+4} \frac{1}{(18)^{\frac{1}{5}} G(0)} (Gr_L^*)^{\frac{1}{5}} \quad (40)$$

3. Mathematical formulation for variable surface temperature

The formulation is similar to that in Section 2 except that power law variation in wall temperature of the form $\bar{T}_w(\bar{x}) - \bar{T}_\infty = b\bar{x}^n$ is assumed, where b is a dimensional constant and n is an exponent. The case of uniform wall temperature corresponds to $n = 0$. We introduce the following non-dimensional variables given by

$$\begin{aligned} x &= \frac{\bar{x}}{L}, & y &= \frac{\bar{y}}{\delta_{wt}} = \left(Gr_L^{\frac{1}{5}}\right) \frac{\bar{y}}{L}, & u_{wt} &= \frac{\bar{u}}{\bar{u}_{0wt}} = \left(Gr_L^{-\frac{2}{5}}\right) \frac{L}{\nu} \bar{u}, \\ v_{wt} &= \frac{\bar{v}}{\varepsilon \bar{u}_{0wt}} = \left(Gr_L^{-\frac{1}{5}}\right) \frac{L}{\nu} \bar{v}, & \theta_{wt} &= \frac{(\bar{T} - \bar{T}_\infty)}{\Delta \bar{T}_{wt}} = \frac{(\bar{T} - \bar{T}_\infty)}{bL^n}, \\ p_{wt} &= \frac{(\bar{p} - \bar{p}_\infty)}{\rho \bar{u}_{0wt}^2} = \left(Gr_L^{-\frac{4}{5}}\right) \frac{(\bar{p} - \bar{p}_\infty)}{\frac{\rho \nu^2}{L^2}}. \end{aligned} \quad (41)$$

The derivation of appropriate velocity scale \bar{u}_{0wt} and the length scale in the \bar{y} -direction δ_{wt} is given in Appendix A. Here Gr_L is the Grashof number given by $Gr_L = \frac{g\beta(\bar{T}_w(L) - \bar{T}_\infty)L^3}{\nu^2}$ (it is to be remembered that Eq. (6) represented the non-dimensionalization when the wall heat flux was prescribed).

The governing non-dimensional boundary layer equations take the same form as presented in (7)–(10) whereas the pertinent boundary conditions become:

$$\begin{aligned} \text{at } y = 0, & \quad u_{wt} = 0, \quad v_{wt} = 0, \quad \theta_{wt} = -x^n, \\ \text{as } y \rightarrow \infty, & \quad u_{wt} \rightarrow 0, \quad \theta_{wt} \rightarrow 0, \quad p_{wt} \rightarrow 0. \end{aligned} \quad (42)$$

Following the same process of stretching transformation as used above in Section 2, the appropriate similarity variable η_{wt} and the functional forms for ψ_{wt} , θ_{wt} and p_{wt} can then be written as:

$$\begin{aligned} \eta_{wt} &= Ax^{\frac{(n-2)}{5}}, & \psi_{wt} &= Bx^{\frac{(n+3)}{5}} f(\eta_{wt}), & \theta_{wt} &= Cx^n g(\eta_{wt}), \\ p_{wt} &= Dx^{\frac{(4n+2)}{5}} h(\eta_{wt}), \end{aligned} \quad (43)$$

where A , B , C and D are positive constants. For $A = B = C = D = 1$, substitution of (43) into the boundary layer equations gives the following set of ordinary differential equations:

$$5f''' - (2n+1)f'^2 + (n+3)ff'' - (4n+2)h - (n-2)\eta_{wt}h' = 0, \quad (44)$$

$$g - h' = 0, \quad (45)$$

$$\frac{5}{Pr}g'' - 5nf'g - (n+3)fg' = 0. \quad (46)$$

The corresponding boundary conditions are:

$$\begin{aligned} \text{at } \eta_{wt} = 0 \text{ and } \eta_{wt} \rightarrow \infty, & \quad f'(0) = f(0) = g(0) - 1 \\ & \quad = f'(\infty) = g(\infty) = h(\infty) = 0. \end{aligned} \quad (47)$$

Following the methods shown in Section 2, the local Nusselt number Nu_x , the wall shear stress τ_w , local skin friction coefficient c_{f_x} , average skin friction coefficient (\hat{c}_f) and the average Nusselt number (\hat{Nu}) can be found out to be:

$$Nu_x = -g'(0)(Gr_x^{\frac{1}{5}}), \quad (48)$$

$$\tau_w = \frac{\mu\nu}{\bar{x}^2} (Gr_x^{\frac{3}{5}}) f''(0), \quad (49)$$

$$c_{f_x} = 2x^{\frac{2}{5}(2n+1)} (Gr_x^{\frac{1}{5}}) f''(0), \quad (50)$$

$$\hat{c}_f = \frac{10}{(3n+4)} (Gr_L)^{-\frac{1}{5}} f''(0), \quad (51)$$

$$\hat{Nu} = -\frac{5}{n+3} (Gr_L)^{\frac{1}{5}} g'(0). \quad (52)$$

4. Method of solution

The system of Eqs. (29)–(31) for power law variation of heat flux, subject to boundary conditions (32), and the system of Eqs. (43)–(45) for power law variation in wall temperature subject to boundary conditions (47) are solved numerically for various values of Pr and m or n using the shooting method. In this method, the system of Eqs. (29)–(31) or (44)–(46) are first reduced to a system of six first order equations. The equations can now be solved by marching forward in η , if the boundary values which are not specified at $\eta = 0$ are first guessed so that the solution process can proceed. However, the boundary values computed at $\eta \rightarrow \infty$ will depend on these guessed values and, in general, will not agree with the actual prescribed conditions at $\eta \rightarrow \infty$. Since we need to guess multiple (three) values simultaneously at $\eta = 0$ for the six first order equations (three boundary conditions prescribed at $\eta \rightarrow \infty$), the Newton method for simultaneous non-linear equations [20] has been used here for finding the roots of the boundary residuals (difference between the computed and specified boundary values at $\eta \rightarrow \infty$). The fourth-order Runge–Kutta method with step size of 0.05 was chosen for the integration of differential equations.

5. Results and discussion

Fig. 2 shows the evolution of the velocity profiles in the x and y directions as the boundary layer due to natural convection

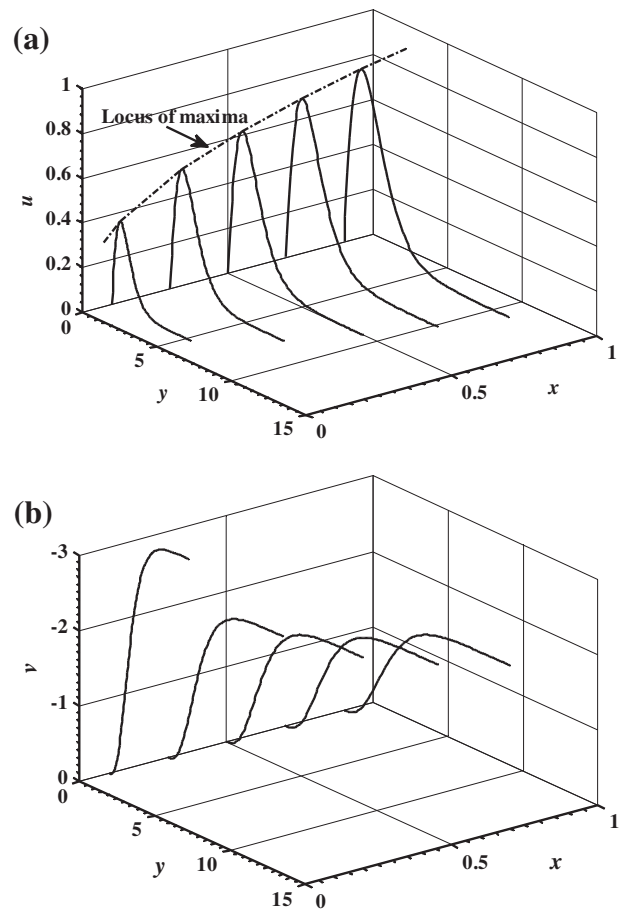


Fig. 2. (a) Predictions of the present theory showing the variation of non-dimensional velocity u versus non-dimensional vertical coordinate y at various distances x along the plate for $Pr = 0.7$ and $m = 0$; $q_w(\bar{x}) = a\bar{x}^m$. (b) Predictions of the present theory showing the variation of non-dimensional velocity v versus non-dimensional vertical coordinate y at various distances x along the plate for $Pr = 0.7$ and $m = 0$; $q_w(\bar{x}) = a\bar{x}^m$.

develops (see Fig. 1). These are the solutions of the equation set (29)–(31) for $Pr = 0.7$ and $m = 0$ (i.e. constant heat flux case). Fig. 2(a) shows that the non-dimensional velocity u is zero on the surface as well as at the edge of the boundary layer (asymptotically) with its maximum occurring at an intermediate value of y . The locus of the maximum u is also shown on the graph. It is seen that the y location of the point for maximum u increases as x increases. Fig. 2(b) shows that the non-dimensional velocity in the y -direction, v , is zero on the surface (the wall being impermeable) but, at a particular x , its magnitude increases continuously with y until a plateau is obtained. The plateau value for v decreases slowly with increasing x . A non-zero value for v at the edge of the boundary layer is physically consistent, as this represents entrainment of previously unaffected fluid. The locus of the end-points of the u -velocity profiles shown in Fig. 2(a) represents how the boundary layer grows in the x -direction.

The characteristic numerical values of $G(0)$ and $F''(0)$ on a uniform heat flux surface for different values of Pr are given in Table 1. According to Eq. (34), the local Nusselt number Nu_x is inversely proportional to $G(0)$, and according to Eq. (35) the wall shear stress τ_w is proportional to $F''(0)$. It is to be noted that both $G(0)$ and $F''(0)$ depend only on Pr and m . From Table 1 it may be concluded that for a fixed value of m , both the skin friction coefficient and the reciprocal of heat transfer coefficient decreases with increase in Pr .

Table 2 presents the values of skin friction coefficient and reciprocal of heat transfer coefficient for various values of m when $Pr = 1$. Inspection of Table 2 reveals that for a given Pr , both the skin friction coefficient and the reciprocal of heat transfer coefficient decreases as the value of m increases. The rate of decrease of both diminishes as m is increased. Thus the wall shear stress decreases nominally while heat transfer rate increases as m is increased for a fixed Pr . Table 3 presents the values of $G(0)$ and $F''(0)$ for various values of Pr when $m = 2$. Table 4 presents the values of skin friction coefficient and reciprocal of heat transfer coefficient for various values of m when $Pr = 7$. Tables 1–4 are constructed when the surface heat flux is specified as a boundary condition.

The characteristic numerical values of $-g'(0)$ and $f''(0)$ on a horizontal surface with constant wall temperature for different values of Pr are given in Table 5. For the general boundary condition in

Table 1
Values of $G(0)$ and $F''(0)$ in Eqs. (34) and (35) for a constant heat flux plate for various values of Pr .

Pr	$G(0)$	$F''(0)$
0.01	3.65580	10.245000
0.1	1.88540	3.062400
0.7	1.18430	1.095500
1	1.09790	0.910070
7	0.75055	0.340530
10	0.70289	0.285220
100	0.46798	0.090971
1000	0.32039	0.028713

Table 2
Values of $G(0)$ and $F''(0)$ in Eqs. (34) and (35) for various values of m when $Pr = 1$.

m	$G(0)$	$F''(0)$
1	0.84793	0.86197
3	0.66415	0.84172
5	0.57789	0.83625
10	0.47213	0.83149
20	0.38301	0.82607
50	0.28395	0.82605
100	0.22987	0.81580

Table 3
Values of $G(0)$ and $F''(0)$ in Eqs. (34) and (35) for $m = 2$ and various values of Pr .

Pr	$G(0)$	$F''(0)$
0.01	2.29550	9.727700
0.1	1.22870	2.879500
0.7	0.79299	1.020000
7	0.51925	0.313800
100	0.32847	0.082724

Table 4
Values of $G(0)$ and $F''(0)$ in Eqs. (34) and (35) for various values of m when $Pr = 7$.

m	$G(0)$	$F''(0)$
1	0.59092	0.31910
3	0.46701	0.30963
5	0.41447	0.30803
10	0.33569	0.30693
20	0.27217	0.30567
50	0.20522	0.30315
100	0.16890	0.29399

Table 5
Values of $g'(0)$ and $f''(0)$ in Eqs. (48) and (49) for an isothermal plate for various values of Pr .

Pr	$-g'(0)$	$f''(0)$
0.01	0.087650	3.921867
0.1	0.196149	2.027907
0.7	0.354304	0.987531
1	0.389570	0.861390
7	0.623621	0.413872
10	0.677046	0.361854
100	1.089644	0.146055
1000	1.747600	0.058810

which the surface temperature is specified (of which constant wall temperature is a special case), the local Nusselt number Nu_x is proportional to $-g'(0)$, according to Eq. (48), and the wall shear stress τ_w is proportional to $f''(0)$, according to Eq. (49). It is to be noted that both $-g'(0)$ and $f''(0)$ depend only on Pr and n . Table 5 shows that, as the Prandtl number of the fluid increases, the magnitude of heat transfer coefficient increases whereas the skin friction coefficient decreases. It can be recalled that this behavior is also observed when the plate is subjected to constant heat flux (Table 1).

The numerical values of heat transfer coefficient $-g'(0)$ and skin friction coefficient $f''(0)$ for a plate subjected to variable wall temperature for various values of n at a fixed Prandtl number is given in Table 6. An increase in n results in an increase in both skin friction coefficient and heat transfer coefficient.

From Eq. (22), one can show that the non-dimensional velocity in the x -direction $\partial\psi/\partial y$ is proportional to $F'(\eta)(\partial\psi/\partial y = ABx^{\frac{m-1}{3}}F'(\eta))$, where the constants A and B are given by Eq. (28)). Fig. 3 presents $F'(\eta)$ for a uniform heat flux surface for various

Table 6
Values of $g'(0)$ and $f''(0)$ in Eqs. (48) and (49) for various values of n when $Pr = 1$.

n	$-g'(0)$	$f''(0)$
1	0.646671	0.980503
3	0.932752	1.148485
5	1.122001	1.250802
10	1.457725	1.418496
20	1.922568	1.626085
50	2.762732	1.946709
100	3.640775	2.233779

values of Prandtl number. The figure shows that at a particular value of Pr , $F'(\eta)$ at first increases with η , goes to a maximum and then decreases asymptotically to zero. The velocity gradient at surface is large for small values of Prandtl number, which produces a large skin friction coefficient $F''(0)$. With increasing Prandtl number, the maximum velocity occurs at a smaller value of η as seen from the graph. The velocity profile for the special case of $Pr = 0.7$ as given by Chen et al. [19] is superposed in Fig. 2 for the purpose of comparison.

From Eqs. (22) and (6), one can show that the non-dimensional temperature is represented by $G(\eta)/G(0)$ ($(\bar{T} - \bar{T}_\infty)/(\bar{T}_w - \bar{T}_\infty) = \theta(\eta)/\theta(0) = G(\eta)/G(0)$). Fig. 4 presents the non dimensional temperature profile for an iso-heat flux surface for various values of Prandtl number. It can be seen from the figure that for a fluid with high value of Prandtl number the temperature gradients at wall are very large resulting in a high rate of heat transfer from the plate surface. The temperature profile for the special case of $Pr = 0.7$ as given by Chen et al. [19] is superposed in Fig. 4 for the purpose of comparison.

Fig. 5 presents the non-dimensional velocity profiles $F'(\eta)$ for various values of m when $Pr = 1$. It can be seen that close to the

wall (i.e. at small values of η) the curves for various values of m are almost superposed on one another. The velocity gradient at wall is therefore a very weak function of m : this can also be seen from Table 2 where it is shown that $F''(0)$ changes only slightly for a very large change in m . The wall shear stress therefore changes only slightly with m (this is later shown in Fig. 8 where the skin friction coefficient is plotted). Fig. 6 presents the non-dimensional temperature profile for various values of m when $Pr = 1$. As the value of m increases, the plate is subjected to a higher value of heat flux. The temperature gradient at wall is more for higher values of m as can be seen from the graph as well as from Table 2 (where it can be seen that $G(0)$ decreases approximately by a factor of 4 as m is increased hundredfold.).

Figs. 7 and 8 show the variation of Nusselt number and skin friction coefficient when the surface heat flux is the prescribed quantity. Computations are performed for a wide range of parameters: the Prandtl number is varied from 0.01 to 100, the value of heating index m is varied from 0 (constant heat flux) to 100. Since Eq. (34) shows that $Nu_x \propto (Gr_x^*)^{1/5}$, the composite variable $Nu_x (Gr_x^*)^{-1/5}$ is plotted as the ordinate in Fig. 7: in this way data generated by comprehensive computations can be presented in a concise manner. For the same reasons, for presenting values of skin friction coefficient,

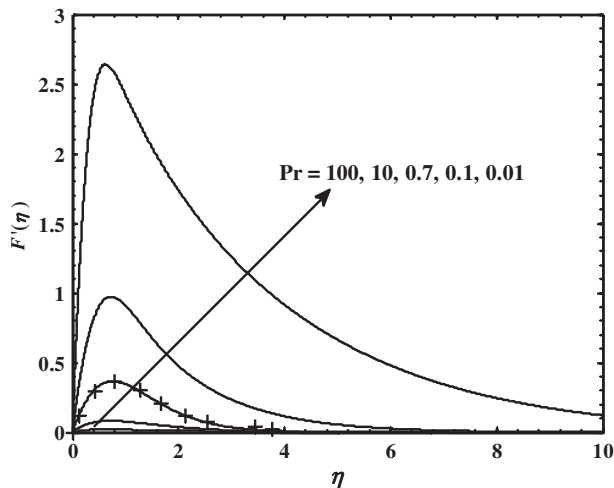


Fig. 3. Non dimensional self-similar velocity profiles for a constant heat flux plate for various values of Pr (— prediction of the present similarity theory; + numerical solutions of integro-differential equations [19]).

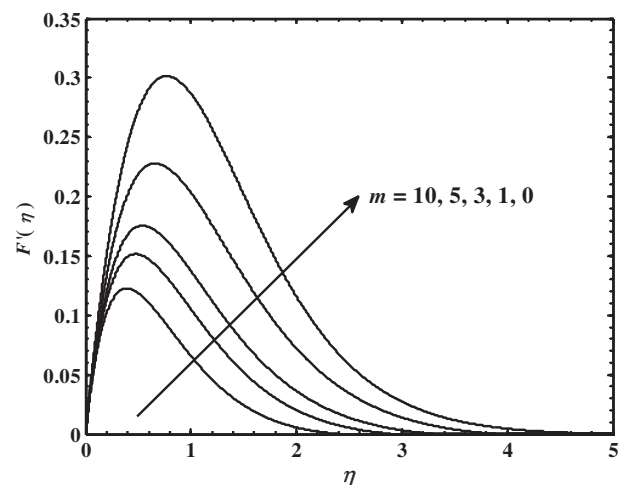


Fig. 5. Non dimensional self-similar velocity profiles for $Pr = 1$ and various values of m ; $q_w(\bar{x}) = a\bar{x}^m$: prediction of the present theory.

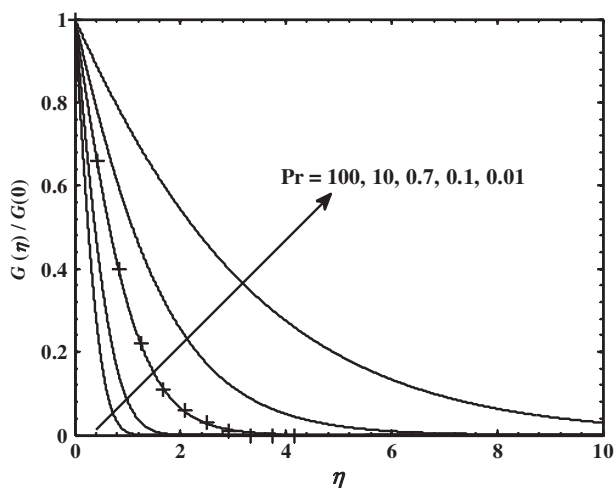


Fig. 4. Non dimensional self-similar temperature profiles for a constant heat flux plate for various values of Pr (— prediction of the present similarity theory; + numerical solutions of integro-differential equations [19]).

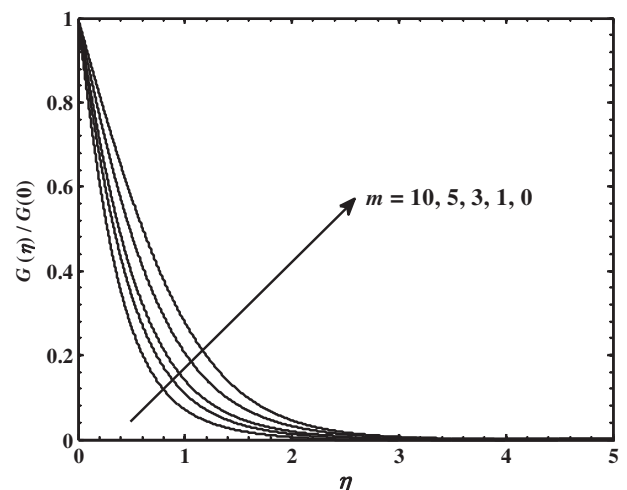


Fig. 6. Non dimensional self-similar temperature profiles for $Pr = 1$ and various values of m ; $q_w(\bar{x}) = a\bar{x}^m$: prediction of the present theory.

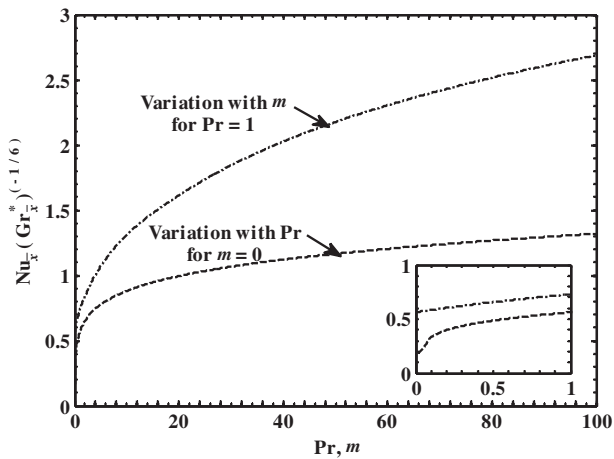


Fig. 7. Prediction of the present theory for the variation in non-dimensional heat transfer coefficient with heating exponent m and Prandtl number Pr ; $q_w(\bar{x}) = a\bar{x}^m$.

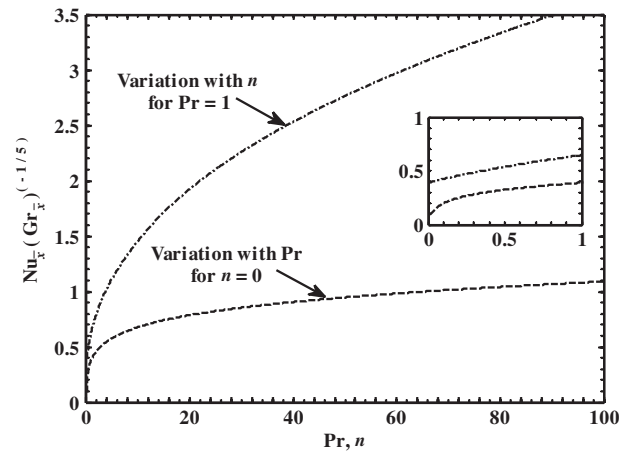


Fig. 9. Prediction of the present theory for the variation in non-dimensional heat transfer coefficient with heating exponent n and Prandtl number Pr ; $\bar{T}_w(\bar{x}) - \bar{T}_\infty = b\bar{x}^n$.

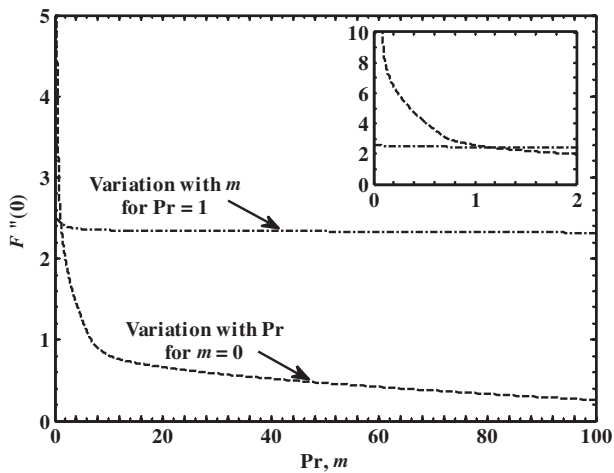


Fig. 8. Prediction of the present theory for the variation in $F''(0)$ giving non-dimensional skin friction coefficient with heating exponent m and Prandtl number Pr ; $q_w(\bar{x}) = a\bar{x}^m$.

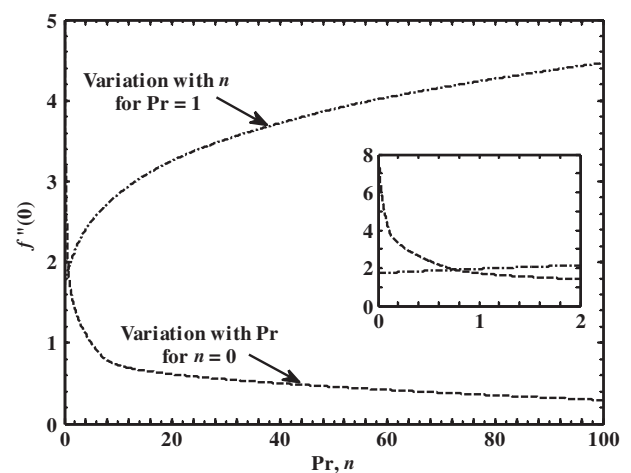


Fig. 10. Prediction of the present theory for the variation in $f''(0)$ giving non-dimensional skin friction coefficient with heating exponent n and Prandtl number Pr ; $\bar{T}_w(\bar{x}) - \bar{T}_\infty = b\bar{x}^n$.

the variable $F''(0)$ is used as the ordinate in Fig. 8. Eqs. (35) and (36) predicts that the wall shear stress as well as the local skin friction factor is directly proportional to $F''(0)$. The computations show that for a particular value of m , the local Nusselt number increases and the local skin friction coefficient decreases with increasing value of Prandtl number for a fixed value of modified Grashof number. Fig. 7 shows that, at fixed values of the modified Grashof number, the Nusselt number increases as the value of m increases for a fixed Prandtl number. Fig. 8, on the other hand, shows that the dependence of local skin friction coefficient on the value of m is very weak. It is interesting to note that this behavior bears resemblance to the case of forced convection where, if constant thermo-physical properties of the fluid are assumed, the skin friction coefficient is determined by the well-known Blasius solution and is completely independent of the value of m .

Equation (40) shows that $\hat{Nu} \propto (Gr_x^*)^{1/6}$; this behavior is exactly the same (except a difference in the constant of proportionality) as that given by $Nu_x \propto (Gr_x^*)^{1/6}$ in equation (34). Thus the conclusions made on the basis of the variation of the local Nusselt number remain valid for the variation of the average Nusselt number as well. Similarly, a study of Eqs. (36) and (38) shows that the variations of the average and local skin friction coefficients follow the same trend.

Figs. 9 and 10 show the variation of Nusselt number and skin friction coefficient when the surface temperature is the prescribed quantity. The trends and qualitative behaviors of these curves are found to be similar to the corresponding behaviors of these curves (Figs. 7 and 8) where the surface heat flux is the prescribed quantity. A comparison of Figs. 8 and 10 shows that the skin friction coefficient depends more strongly on n (i.e. when the surface temperature is prescribed) than on m (i.e. when the surface heat flux is prescribed). A comparison of Figs. 8 and 10 shows that the skin friction coefficient depends more strongly on the Prandtl number when the surface heat flux is constant as compared to the case when the surface temperature is constant.

In order to understand further the mathematical nature of the similarity theory, a series solution of the Eqs. (29)–(31), (44)–(46) following the perturbation method has also been formulated in the present work. A summary of the principal steps for such an analysis, when the plate is subjected to a variable heat flux of the form $q_w(\bar{x}) = a\bar{x}^m$, for two limiting cases – $m \sim 0$ and $m \gg 1$ is given in Appendix B as an example application of the procedure. Figs. 11 and 12 given in Appendix B compare the full numerical solutions of the similarity theory with the approximate first-order series solutions (Eqs. (B6) and (B17)).

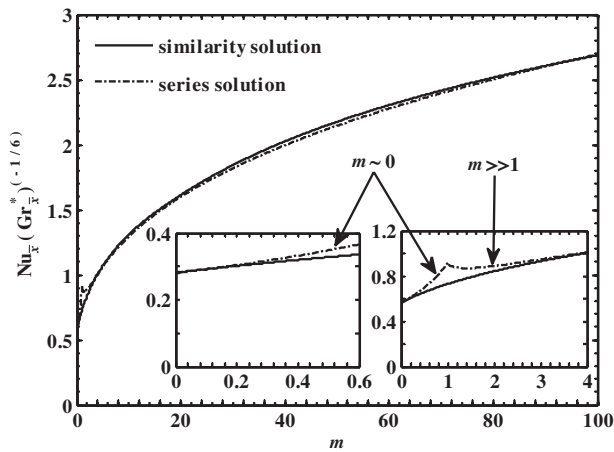


Fig. 11. Prediction of the present theory showing the variation of non-dimensional heat transfer coefficient with heating exponent m for $Pr = 1$; $q_w(\bar{x}) = a\bar{x}^m$ (— full numerical solution of similarity theory; - - - first-order straightforward expansion).

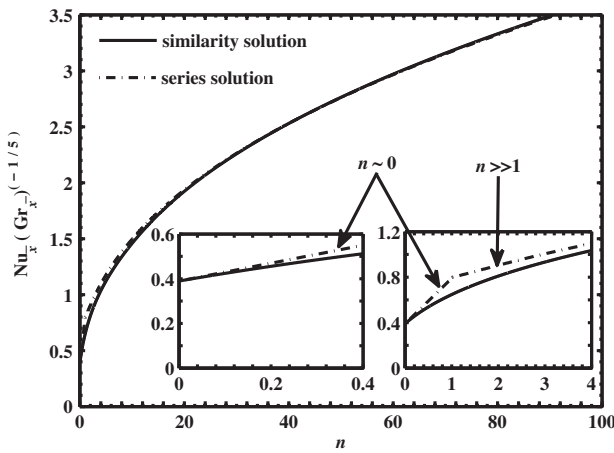


Fig. 12. Prediction of the present theory showing the variation of non-dimensional heat transfer coefficient with heating exponent n for $Pr = 1$; $\bar{T}_w(\bar{x}) - \bar{T}_\infty = b\bar{x}^n$ (— full numerical solution of similarity theory; - - - first-order straightforward expansion).

6. Conclusion

In this paper, an analytical study of the problem of steady, laminar natural convection boundary layer flows over a semi-infinite horizontal flat plate for power law variation in both the surface heat flux and the wall temperature has been made. The procedure of obtaining the similarity variable using generalized stretching transformation for any problem permitting similarity solution is given. Similarity solutions are then formulated for both boundary conditions, viz. $q_w(\bar{x}) = a\bar{x}^m$ and $\bar{T}_w(\bar{x}) = \bar{T}_\infty + b\bar{x}^n$, the fundamental coupled equation sets derived here being Eqs. (29)–(31) and Eqs. (44)–(46), respectively. The particular cases of constant heat flux and constant surface temperature are obtained by respectively substituting $m = 0$ or $n = 0$ in the solutions. Similarity solution for natural convection boundary layers on horizontal semi-infinite plates when the heat flux is the prescribed quantity has been derived for the first time in the present paper: a modified Grashof number Gr_L^* is used for this purpose.

Representative velocity and temperature profiles for $q_w(\bar{x}) = a\bar{x}^m$ are plotted in Figs. 3–6 corresponding to two cases:

(i) for various values of Pr when the heat flux is constant along the surface, and (ii) for various levels of heating (varying m) when the Prandtl number is 1. The present similarity solution agrees well with the solution from the integro-differential approach of Chen et al. [19] who provided solutions only for two cases of heat flux variation for a fixed Prandtl number – $Pr = 0.7$, $m = 0$, and $Pr = 0.7$, $m = 1$.

The systematic procedure for obtaining the similarity solutions for $\bar{T}_w(\bar{x}) = \bar{T}_\infty + b\bar{x}^n$ helps to identify appropriate scales to non-dimensionalize various parameters. The general solution developed here reduces to the specific case for isothermal plates given by Stewartson [15] and Gill et al. [16] by substituting $n = 0$ in the equations.

A systematic study has been made for various values of Prandtl number Pr and the constants m or n . Theoretical relations have been derived here on the variation of Nusselt number (Eqs. (34), (40), (48), (52)) and skin friction coefficient (Eqs. (36), (38), (50), (51)) with the Grashof number (or modified Grashof number). Appropriate velocity scales for the non-dimensionalization of the shear stress are derived in the paper (Eqs. (A7) and (A9) in the Appendix A). Similarly, for the heat flux case, an appropriate temperature scale has also been derived (Eq. (A10) in the Appendix A). The major findings from these studies can be summed up as follows:

- (1) For a fixed value of m or n (including the cases of constant wall temperature or constant heat flux), the heat transfer coefficient increases whereas the local wall shear stress decreases with increasing Prandtl number.
- (2) The heat transfer coefficient increases with increasing values of exponent m or n when the Prandtl number of the fluid is kept constant.
- (3) For a fixed Prandtl number, the local wall shear stress increases with increasing values of n for power law variation in surface temperature while it decreases with increasing values of m for power law variation in heat flux. This is in contrast with the results proposed by Chen et al. [19] where local wall shear stress decreases for both cases.
- (4) The non-dimensional correlations developed in the present work show that the Nusselt number increases but the skin friction coefficient decreases with increasing Grashof number. This is true either when the wall heat flux ($\hat{Nu} \propto (Gr_L^*)^{1/5}$ and $\hat{c}_f \propto (Gr_L^*)^{-1/5}$) or when the wall temperature ($\hat{Nu} \propto (Gr_L^*)^{1/5}$ and $\hat{c}_f \propto (Gr_L^*)^{-1/5}$) is specified.
- (5) The behavior of average Nusselt number and average skin friction coefficient would be similar to that of local Nusselt number and local skin friction coefficient for all the cases that were investigated.

Appendix A. Derivation of appropriate velocity scales for non-dimensionalisation of wall shear stress, and a temperature scale for the case of prescribed heat flux

Consider a steady two-dimensional laminar incompressible flow. The Navier–Stokes equations giving the conservation of mass, momentum and energy in the rectangular Cartesian coordinate system invoking the Boussinesq approximation are well known (e.g. see Refs. [14,18]).

The equations are now non-dimensionalized. The length and the velocity scales are chosen as L and \bar{u}_0 (to be determined), respectively. The non-dimensional variables are:

$$x = \frac{\bar{x}}{L}, \quad \bar{y} = \frac{\bar{y}}{L}, \quad u = \frac{\bar{u}}{\bar{u}_0}, \quad \bar{v} = \frac{\bar{v}}{\bar{u}_0}, \quad \theta = \frac{\bar{T} - \bar{T}_\infty}{\Delta\bar{T}}, \quad p = \frac{\bar{p} - \bar{p}_\infty}{\rho\bar{u}_0^2}. \tag{A1}$$

Table A1
Order of magnitude analysis.

Variable	Appropriate scale		Order of magnitude of non-dimensional variable
	Wall temperature	Heat flux	
\bar{x}	L	L	$x = \bar{x}/L \sim 1$
\bar{y}	$\delta = \varepsilon L$	$\delta_{wt} = \varepsilon L$	$\bar{y} = \bar{y}/L \sim \varepsilon$
\bar{u}	\bar{u}_0	\bar{u}_{0wt}	$u = \bar{u}/\bar{u}_0 \sim 1$
\bar{v}	$\varepsilon \bar{u}_0$	$\varepsilon \bar{u}_{0wt}$	$u = \bar{u}/\bar{u}_{0wt} \sim 1$ $\bar{v} = \bar{v}/\bar{u}_0 \sim \varepsilon$
\bar{p}	$\rho \bar{u}_0^2$	$\rho \bar{u}_{0wt}^2$	$\bar{v} = \bar{v}/\bar{u}_{0wt} \sim \varepsilon$ $p = (\bar{p} - \bar{p}_\infty)/(\rho \bar{u}_0^2) \sim 1$ $p = (\bar{p} - \bar{p}_\infty)/(\rho \bar{u}_{0wt}^2) \sim 1$

$\Delta \bar{T}$ in Eq. (A1) is known from the boundary conditions when wall temperature is prescribed, but needs to be determined when heat flux is the prescribed quantity.

After non-dimensionalisation in the particular way as described above in (A1), the Navier–Stokes equations become:

$$u \frac{\partial u}{\partial x} + \bar{v} \frac{\partial u}{\partial y} = -\frac{\partial p}{\partial x} + \frac{1}{Re_L} \left(\frac{\partial^2 u}{\partial x^2} + \frac{\partial^2 u}{\partial y^2} \right), \tag{A2}$$

$$u \frac{\partial \bar{v}}{\partial x} + \bar{v} \frac{\partial \bar{v}}{\partial y} = -\frac{\partial p}{\partial y} + \frac{Gr_L}{Re_L^2} \theta + \frac{1}{Re_L} \left(\frac{\partial^2 \bar{v}}{\partial x^2} + \frac{\partial^2 \bar{v}}{\partial y^2} \right), \tag{A3}$$

$$u \frac{\partial \theta}{\partial x} + \bar{v} \frac{\partial \theta}{\partial y} = \frac{1}{Re_L Pr} \left(\frac{\partial^2 \theta}{\partial x^2} + \frac{\partial^2 \theta}{\partial y^2} \right). \tag{A4}$$

$$u \frac{\partial \theta}{\partial x} + \bar{v} \frac{\partial \theta}{\partial y} = \frac{1}{Re_L Pr} \left(\frac{\partial^2 \theta}{\partial x^2} + \frac{\partial^2 \theta}{\partial y^2} \right). \tag{A5}$$

In Eq. (A4), Gr_L should be interpreted as the usual Grashof number for the case when wall temperature is known, but should be interpreted as the modified Grashof number Gr_L^* for the case when the wall heat flux is the prescribed quantity.

Now, we can identify the following scales for the boundary layer variables as given in Table A1.

A.1. Determination of the appropriate velocity scale (\bar{u}_0 and \bar{u}_{0wt})

From the y-momentum Eq. (A4) we have:

Inertia force $\sim O(\varepsilon)$,

Viscous force $\sim O\left(\frac{1}{Re_L} \frac{1}{\varepsilon}\right)$.

Now, if the order-of-magnitude of the viscous force has to be the same with that of the inertia force within the boundary layer, then:

$$O(\varepsilon) \approx O\left(\frac{1}{Re_L} \frac{1}{\varepsilon}\right)$$

which gives:

$$\varepsilon \sim \frac{1}{\sqrt{Re_L}}. \tag{A6}$$

A.1.1. Power law variation in wall temperature

For power law variation in wall temperature of the form $\bar{T}_w(\bar{x}) - \bar{T}_\infty = b\bar{x}^n$, the order of magnitude of buoyancy and pressure forces from y-momentum Eq. (A4) gives:

Buoyancy force $\sim O\left(\frac{Gr_L}{Re_L^2}\right)$,

Pressure force $\sim O\left(\frac{1}{\varepsilon}\right)$.

The decreased pressure gradient in y-direction is a consequence of buoyancy force [14]. Hence equating order of magnitude of buoyancy and pressure force in the boundary-layer region one obtains:

$$O\left(\frac{Gr_L}{Re_L^2}\right) \approx O\left(\frac{1}{\varepsilon}\right)$$

which gives $Re_L \approx Gr_L^{\frac{2}{3}}$

$$\text{Hence } \delta_{wt} = \varepsilon L \approx Gr_L^{-\frac{1}{3}} L \text{ and } \bar{u}_{0wt} = \frac{v}{L} (Gr_L)^{\frac{2}{3}}. \tag{A7}$$

This is used in the non-dimensionalisation shown in Eq. (41).

A.1.2. Power law variation in wall heat flux

For power law variation in wall heat flux of the form $q_w(\bar{x}) = a\bar{x}^m$:

$$\theta \sim O(\varepsilon) \text{ as } y \sim O(\varepsilon) \text{ so that } \frac{\partial \theta}{\partial y} \sim O(1). \tag{A8}$$

Buoyancy force $\sim O\left(\frac{Gr_L^*}{Re_L^2} \varepsilon\right)$,

Pressure force $\sim O\left(\frac{1}{\varepsilon}\right)$,

$$O\left(\frac{Gr_L^*}{Re_L^2} \varepsilon\right) \approx O\left(\frac{1}{\varepsilon}\right)$$

which gives $Re_L \approx (Gr_L^*)^{\frac{1}{3}}$

$$\text{Hence } \delta = \varepsilon L \approx (Gr_L^*)^{-\frac{1}{3}} L \text{ and } \bar{u}_0 = \frac{v}{L} (Gr_L^*)^{\frac{1}{3}}. \tag{A9}$$

This is used in the non-dimensionalisation shown in Eq. (6).

A.2. Determination of the appropriate temperature scale ($\Delta \bar{T}$)

When the surface temperature is prescribed then the temperature scale for non-dimensionalisation is obvious: it is taken as $\Delta \bar{T}_{wt} = \bar{T}_w(L) - \bar{T}_\infty$, as used in Eq. (41). However, when the surface heat flux is prescribed, an appropriate temperature scale has to be derived as follows:

$$\text{at } \bar{y} = 0, \quad -k \frac{\partial \bar{T}}{\partial y} = a\bar{x}^m,$$

$$-k \frac{\Delta \bar{T}}{L} \frac{\partial \theta}{\partial y} = aL^m \bar{x}^m,$$

$$\text{Choose } \Delta \bar{T} = \frac{aL^m L}{k} = \frac{q_w(L)L}{k}, \tag{A10}$$

so that at $y = 0, \frac{\partial \theta}{\partial y} = -\bar{x}^m$.

This temperature scale $\Delta \bar{T}$ is used in the non-dimensionalisation shown in Eq. (6).

Appendix B. Application of perturbation methods to free convection flow

Further insight to the mathematical nature of the solution can be obtained by applying first-order straightforward expansion of perturbation technique. A concise analysis is presented below for free convection over a horizontal plate when the heat flux is prescribed for two limiting cases: $m \sim 0$ and $m \gg 1$.

Case 1: $m \sim 0$

An approximate solution of Eqs. (29)–(31) subject to the boundary conditions (32), near $m \sim 0$ can be obtained by expanding $F(\eta)$, $H(\eta)$ and $G(\eta)$ in a power series in m of the form:

$$\left. \begin{aligned} F(\eta) &= F_0(\eta) + mF_1(\eta) + \dots \\ H(\eta) &= H_0(\eta) + mH_1(\eta) + \dots \\ G(\eta) &= G_0(\eta) + mG_1(\eta) + \dots \end{aligned} \right\} \quad (B1)$$

Substituting the expansions (B1) into Eqs. (29)–(31) and boundary conditions (32) and equating coefficients of equal powers of m lead to the following two systems of equations (denoted below by the Equation sets (B2) and (B4) respectively):

$$\left. \begin{aligned} F_0''' + 4F_0F_0'' - 2F_0'^2 + \eta H_0' - 2H_0 &= 0 \\ H_0' &= G_0 \\ \frac{1}{Pr} G_0'' + 4F_0G_0' - 2F_0'G_0 &= 0 \end{aligned} \right\}, \quad (B2)$$

subject to the boundary conditions:

$$F_0'(0) = F_0(0) = 1 + G_0'(0) = F_0'(\infty) = G_0(\infty) = H_0(\infty) = 0, \quad (B3)$$

and

$$\left. \begin{aligned} F_1''' + 4F_0F_1'' - 4F_0'F_1' + 4F_0''F_1 + \eta H_1' - 2H_1 + F_0F_0'' - 2F_0'^2 - \frac{1}{2}\eta H_0' - 2H_0 &= 0 \\ H_1' &= G_1 \\ \frac{1}{Pr} G_1'' + 4F_0G_1' - 2F_0'G_1 - 2G_0F_1' + 4G_0'F_1 + G_0'F_0 - 5F_0'G_0 &= 0 \end{aligned} \right\}, \quad (B4)$$

subject to the boundary conditions:

$$F_1'(0) = F_1(0) = G_1'(0) = F_1'(\infty) = G_1(\infty) = H_1(\infty) = 0. \quad (B5)$$

Solving both sets of Eqs. (B2) and (B4) numerically, subject to the appropriate boundary conditions (B3) and (B5), for $Pr = 1$ gives:

$$\left. \begin{aligned} F''(0) &= 0.908231 - 0.098472m + \dots \\ G(0) &= 1.101024 - 0.428537m + \dots \end{aligned} \right\}. \quad (B6)$$

Equation set (B6) constitutes the solution for $m \sim 0$.

Case 2: $m \gg 1$

For large values of $m(\gg 1)$, solution of Eqs. (29)–(31) subject to the boundary conditions (32) can be obtained by making the following transformation:

$$\left. \begin{aligned} \xi &= m^{\frac{1}{3}}\eta, \quad F(\eta) = m^{-\frac{2}{3}}\tilde{F}(\xi), \quad H(\eta) = m^{-\frac{2}{3}}\tilde{H}(\xi) \quad \text{and} \quad G(\eta) \\ &= m^{-\frac{1}{3}}\tilde{G}(\xi). \end{aligned} \right\} \quad (B7)$$

This leads to the equations:

$$\left. \begin{aligned} \tilde{F}''' - 2 \left[\left(1 + \frac{1}{m}\right) \tilde{F}'^2 - \left(1 + \frac{4}{m}\right) \frac{1}{2} \tilde{F} \tilde{F}'' \right] \\ - \left[2 \left(1 + \frac{1}{m}\right) \tilde{H} + \frac{1}{2} \left(1 - \frac{2}{m}\right) \xi \tilde{H}' \right] &= 0, \end{aligned} \right\} \quad (B8)$$

$$\tilde{G} - \tilde{H}' = 0, \quad (B9)$$

$$\frac{1}{Pr} \tilde{G}'' - \left[\left(5 + \frac{2}{m}\right) \tilde{F}' \tilde{G} - \left(1 + \frac{4}{m}\right) \tilde{F} \tilde{G}' \right] = 0. \quad (B10)$$

The corresponding boundary conditions are:

$$\tilde{F}'(0) = \tilde{F}(0) = 1 + \tilde{G}'(0) = \tilde{F}'(\infty) = \tilde{G}(\infty) = \tilde{H}(\infty) = 0, \quad (B11)$$

where primes now denote differentiation with respect to ξ .

A solution of Eqs. (B8)–(B10) subject to the boundary conditions (B11) is sought to be of the form:

$$\left. \begin{aligned} \tilde{F}(\xi) &= \tilde{F}_0(\xi) + \frac{1}{m} \tilde{F}_1(\xi) + \dots \\ \tilde{H}(\xi) &= \tilde{H}_0(\xi) + \frac{1}{m} \tilde{H}_1(\xi) + \dots \\ \tilde{G}(\xi) &= \tilde{G}_0(\xi) + \frac{1}{m} \tilde{G}_1(\xi) + \dots \end{aligned} \right\}, \quad (B12)$$

where $\tilde{F}_0, \tilde{H}_0, \tilde{G}_0$ and $\tilde{F}_1, \tilde{H}_1, \tilde{G}_1$ are the solution of the differential equations (denoted below by the equation sets (B13) and (B15), respectively):

$$\left. \begin{aligned} \tilde{F}_0''' + \tilde{F}_0 \tilde{F}_0'' - 2\tilde{F}_0'^2 - \frac{1}{2} \xi \tilde{H}_0' - 2\tilde{H}_0 &= 0 \\ \tilde{H}_0' &= \tilde{G}_0 \\ \frac{1}{Pr} \tilde{G}_0'' + \tilde{F}_0 \tilde{G}_0' - 5\tilde{F}_0' \tilde{G}_0 &= 0 \end{aligned} \right\}, \quad (B13)$$

subject to the boundary conditions:

$$\left. \begin{aligned} \tilde{F}_0'(0) = 0, \quad \tilde{F}_0(0) = 0, \quad 1 + \tilde{G}_0'(0) = 0 \\ \tilde{F}_0'(\infty) = 0, \quad \tilde{G}_0(\infty) = 0, \quad \tilde{H}_0(\infty) = 0 \end{aligned} \right\}, \quad (B14)$$

and,

$$\left. \begin{aligned} \tilde{F}_1''' + \tilde{F}_0 \tilde{F}_1'' - 4\tilde{F}_0' \tilde{F}_1' + \tilde{F}_0'' \tilde{F}_1 - \frac{1}{2} \xi \tilde{H}_1' - 2\tilde{H}_1 + 4\tilde{F}_0 \tilde{F}_0'' - 2\tilde{F}_0'^2 + \xi \tilde{H}_0' - 2\tilde{H}_0 &= 0 \\ \tilde{H}_1' &= \tilde{G}_1 \\ \frac{1}{Pr} \tilde{G}_1'' + \tilde{F}_0 \tilde{G}_1' - 5\tilde{F}_0' \tilde{G}_1 - 5\tilde{G}_0 \tilde{F}_1' + \tilde{G}_0' \tilde{F}_1 + 4\tilde{G}_0' \tilde{F}_0 - 2\tilde{F}_0' \tilde{G}_0 &= 0 \end{aligned} \right\}, \quad (B15)$$

subject to the boundary conditions:

$$\left. \begin{aligned} \tilde{F}_1'(0) = 0, \quad \tilde{F}_1(0) = 0, \quad \tilde{G}_1'(0) = 0 \\ \tilde{F}_1'(\infty) = 0, \quad \tilde{G}_1(\infty) = 0, \quad \tilde{H}_1(\infty) = 0 \end{aligned} \right\}. \quad (B16)$$

Numerical solution of both sets of Eqs. (B13) and (B15), subject to the appropriate boundary conditions (B14) and (B16), for $Pr = 1$ gives:

$$\left. \begin{aligned} F''(0) &= 0.816449 + m^{-1}0.069319 + \dots \\ G(0) &= m^{-\frac{1}{3}}(1.068595 - m^{-1}0.383858 + \dots) \end{aligned} \right\}. \quad (B17)$$

Equation set (B17) therefore constitutes the solution for $m \gg 1$.

A similar analysis has been carried out for $n \sim 0$ and $n \gg 1$ when the surface temperature is prescribed instead of heat flux. The calculations pertaining to the case of variable surface temperature is not repeated here for brevity, but the results have been included in Fig. 12. The solutions for $Nu_{\tilde{x}}(Gr_{\tilde{x}}^*)^{-\frac{1}{6}}$ (with prescribed heat flux) and for $Nu_{\tilde{x}}(Gr_{\tilde{x}})^{-\frac{1}{3}}$ (with prescribed surface temperature) are obtained from the full numerical solution of the similarity theory and the approximate series solution are compared in Figs. 11 and 12 respectively. It is found that the two methods are in reasonable agreement even for moderate values of m or n .

References

- [1] V.S.V. Rajan, J.J.C. Picot, Experimental study of the laminar free convection from a vertical plate, *Ind. Eng. Chem. Fund.* 10 (1) (1971) 132–134.
- [2] L.C. Burmeister, *Convective Heat Transfer*, John Wiley and Sons, New York, 1983.
- [3] O.G. Martynenko, A.A. Berezovsky, Yu.A. Sokovishin, Laminar free convection from a vertical plate, *Int. J. Heat Mass Transfer* 27 (6) (1984) 869–881.
- [4] O.G. Martynenko, P.P. Khramtsov, *Free Convective Heat Transfer: With Many Photographs of Flows and Heat Exchange*, Springer, New York, 2005.
- [5] K.K. Sharma, M. Adelman, Experimental study of natural convection heat transfer from a vertical plate in a non-Newtonian fluid, *Can. J. Chem. Eng.* 47 (6) (1969) 553–555.

- [6] S. Ghosh Moulic, L.S. Yao, Non-Newtonian natural convection along a vertical flat plate with uniform surface temperature, *J. Heat Transfer* 131 (6) (2009) 1–8.
- [7] V.N. Kurdyumov, Natural convection near an isothermal wall far downstream from a source, *Phys. Fluids* 17 (8) (2005) 1–8.
- [8] R.J. Goldstein, K.S. Lau, Laminar natural convection from a horizontal plate and the influence of plate-edge extensions, *J. Fluid Mech.* 129 (1983) 55–75.
- [9] H.K. Kuiken, Free convection at low Prandtl numbers, *J. Fluid Mech.* 37 (Pt 4) (1969) 785–798.
- [10] J.V. Clifton, A.J. Chapman, Natural convection on a finite size horizontal plate, *Int. J. Heat Mass Transfer* 12 (12) (1984) 1573–1584.
- [11] S. Pretot, B. Zeghmati, G. Le Palec, Theoretical and experimental study of natural convection on a horizontal plate, *Appl. Therm. Eng.* 20 (10) (2000) 873–891.
- [12] R.L. Mahajan, B. Gebhart, Higher order boundary layer effects in plane horizontal natural convection flows, *J. Heat Transfer* 102 (2) (1980) 368–371.
- [13] N. Afzal, Higher order effects in natural convection flow over a uniform flux horizontal surface, *Wärme -und Stoffübertragung* 19 (3) (1985) 177–180.
- [14] H. Schlichting, K. Gersten, *Boundary-Layer Theory*, Springer, New Delhi, 2004.
- [15] K. Stewartson, On the free convection from a horizontal plate, *Z. Angew. Math. Phys. ZAMP* 9 (3) (1958) 276–282.
- [16] W.N. Gill, D.W. Zeh, E. Del Casal, Free convection on a horizontal plate, *Z. Angew. Math. Phys. ZAMP* 16 (4) (1965) 539–541.
- [17] Z. Rotem, L. Claassen, Natural convection above unconfined horizontal surfaces, *J. Fluid Mech.* 38 (pt 1) (1969) 173–192.
- [18] B. Gebhart, Y. Jaluria, R.L. Mahajan, B. Sammakia, *Buoyancy-Induced Flows and Transport*, Hemisphere Publishing Corporation, New York, 1988.
- [19] T.S. Chen, H.C. Tien, B.F. Armaly, Natural convection on horizontal, inclined and vertical plates with variable surface temperature or heat flux, *Int. J. Heat Mass Transfer* 29 (10) (1986) 1465–1478.
- [20] B. Bradie, *A Friendly Introduction to Numerical Analysis*, Pearson Education, New Delhi, 2007.